JACC Vol. 11, No. 1
January 1988:177-85

EXPERIMENTAL STUDIES

Disproportionate Epicardial Dilation After Transmural Infarction of the Canine Left Ventricle: Acute and Chronic Differences

DAVID A. KASS, MD, W. LOWELL MAUGHAN, MD, ALLEN CIUFFO, MD, WILLARD GRAVES, PHD, BERNADINE HEALY, MD, FACC, MYRON L. WEISFELDT, MD, FACC
Baltimore, Maryland

The relation between acute disproportionate infarct dilation and late postinfarct left ventricular remodeling was examined by implanting multiple radiopaque epicardial markers in the left ventricle of eight dogs and determining regional surface deformation after acute and chronic transmural infarction. Transmural injury was produced by combining coronary ligation with distal embolization of a rubber polymer. Dogs were anesthetized and studied before and 1 h, 24 h and 1 week after infarction. Marker positions were recorded by rapid biplane cineradiography, and three-dimensional coordinates were reconstructed by a computer-assisted tracking system. Regional deformation was expressed by a local surface area equal to the sum of multiple (three to four) triangles generated by marker triplets.

As early as 1 h after infarction, end-diastolic area in the infarct region increased by 20.3 ± 3.1%, while that in the remote region increased by only 7.9 ± 3.5%. Both changes and the difference between them were significant. At 24 h after infarction, both territories continued to undergo dilation, this time to a similar extent (additional +10.3% in the remote region and +10.1% in the infarct region), thus maintaining the significant disproportionate infarct dilation. At 1 week, however, the infarct territory remained dilated with a mean end-diastolic area 31.4 ± 3.1% above control, while that in the remote region returned to a net mean 8.5 ± 4.7% increase.

Thus, the major extent of disproportionate infarct dilation occurs within 1 h after transmural injury and is accompanied by remote dilation as a compensatory response. The extent of further infarct dilation achieved by 24 h is maintained in the chronic infarct, and compensatory mechanisms enable noninjured myocardium to become less dilated. This is an even earlier time course than previously demonstrated, which suggests that attempts to limit infarct dilation should target the acute phase of injury.

(J Am Coll Cardiol 1988;11:177-85)

Transmural myocardial infarction of the left ventricle frequently results in generalized as well as disproportionate regional infarct dilation (1–5). Global chamber enlargement enhances stroke volume by the Frank-Starling mechanism and helps maintain cardiac output in the presence of ischemic injury (6–10). Infarct expansion, however, is regarded as disadvantageous because it distorts chamber geometry (2,3,11), is associated with reduced overall ventricular function (11,12) and may lead to myocardial wall rupture (13). Clinical studies (13–15) have demonstrated that patients with marked regional infarct dilation have a poor prognosis.

Although postmortem studies in the rat (1,2,16) and clinical data (14) have shown that disproportionate infarct dilation can be present as early as 24 h after injury, studies in models of acute ischemia (4,6–9) suggest that this could occur earlier in the acute phase of the injury. However, most acute and chronic models of canine infarction (17–21) have utilized coronary ligation, a technique that generally does not produce transmural injury, which is an important substrate for the development of infarct expansion (5,22,23). Thus, despite these previous studies, there are still few in vivo data that relate early (within 1 to 2 h) regional dilation

From the Division of Cardiology, Department of Medicine, The Johns Hopkins Medical Institutions, Baltimore, Maryland. Dr. Healy's present address is: Research Division, The Cleveland Clinics, Cleveland, Ohio 44106. This study was supported by National Health Service Grants HL-4529, HL-4903 and HL-33243 from the National Institutes of Health, Bethesda, Maryland. Dr. Kass is a recipient of Physician Scientist Award HL-01820 and Dr. Maughan is a recipient of Research Career Development Award HL-01610-01 from the National Institutes of Health.

Manuscript received April 21, 1987; revised manuscript received July 23, 1987, accepted August 7, 1987.

Address for reprints: David A. Kass, MD, Division of Cardiology, Carnegie 565A, Johns Hopkins Medical Institutions, 600 North Wolfe Street, Baltimore, Maryland 21205.

0735-1097/88/$3.50

JACC Vol. 11, No. 1
January 1988:177-85

changes to late ventricular remodeling after transmural infarction.

Ideally, to accurately relate early and late regional deformation changes in vivo, multiple discrete points in the myocardium should be examined over time. With echocardiographic imaging, it is difficult to maintain a precise and reproducible position of the transducer beam, particularly if the geometry of internal landmarks (such as papillary muscles) is altered with infarction. Sonomicrometry provides sensitive dimension measurements; however, this approach is limited by the number of sensors that can be implanted and thus has been used primarily to define single segment lengths.

In the present study, we implanted multiple radiopaque markers in the epicardium of the canine left ventricle and determined their three-dimensional positions using high speed biplane cineradiography. This provided precise surface deformation data in both remote and infarct regions. Using a model of transmural infarction, we determined whether the largest disparities between the dilation of infarcted versus normal remote myocardium occurred in the acute phase or later after the onset of injury. In addition, the influence these initial changes had on ventricular remodeling were observed at 1 week after infarction.

Methods

Surgical preparation. Eight adult mongrel dogs weighing 20 to 30 kg were anesthetized with sodium pentobarbital (30 mg/kg body weight) and ventilated using a constant volume respirator (Harvard Apparatus, model 613). Succinylcholine was given intravenously (20 mg), and the chest was opened through a lateral thoracotomy incision. The internal mammary vein was cannulated for drug administration. The left atrium was cannulated with an indwelling guiding tube to permit introduction of a 5F high fidelity micromanometer-tipped catheter (Millar, model PC 350) into the left ventricle.

Multiple (mean number = 15) 1 mm stainless steel spherical beads were introduced into the epicardial layer using a vacuum suction-needle apparatus, as previously described (24). These beads were placed throughout both remote and what were to become infarcted territories, with an interbead distance of 1 to 2 cm. The markers were visible on the surface of the heart in nearly all instances. This aspect was a major reason for choosing epicardial placement because it facilitated eventual matching of the computer-calculated marker positions and the actual markers on the heart. Tissue fibrosis around the beads has been shown to be minimal with this bead implantation technique (24), with perimarker fibrosis extending at most by 0.1 mm from the outer bead surface.

Experimental protocol. Once the markers were implanted, the chest was closed and air was evacuated. After 1 to 2 h for stabilization, the control study was performed while the animal remained anesthetized. The pressure transducer catheter was introduced into the left ventricle through the left atrial cannula. Zero reference was taken at the level of the mid left ventricle and calibrated using an electronic reference signal preset by comparison with a mercury manometer. Calibration was performed before and after each study and varied by less than 2 mm Hg. An electrocardiogram (ECG) was simultaneously recorded using limb leads. Biplane cineradiograms were then taken at a rate of 90 frames/s (General Electric, model MSI 850-II), with simultaneous recordings of left ventricular pressure. Synchronization of the cine frames with pressure was provided by recording an analog square wave signal synchronized with the X-ray beam pulse.

After baseline cineangiographic and pressure recordings were obtained, the dogs were returned to the surgical suite. The chest was reopened and the mid circumflex artery or its first large obtuse marginal branch was isolated in six dogs, and the mid left anterior descending artery was isolated in two. Intravenous lidocaine (1 mg/kg) was administered prophylactically, the isolated vessel was ligated and the distal lumen was injected with 1 ml of a biologically inert, nonresorptive, polysulfide polymer (Sybron/Kerr Laboratories). This material, premixed with a catalyst, achieved a soft rubbery consistency within 20 s. This technique of coronary ligation and embolization has previously been demonstrated (5) to produce consistent moderate-sized transmural infarction. The dog was allowed to stabilize for 20 min after coronary occlusion. Additional lidocaine (20 mg bolus) was occasionally required after occlusion to control ventricular ectopic activity.

All indwelling lines were externalized between the scapulae. The chest was closed in two layers and air was evacuated. Repeat cineradiograms and synchronized pressure recordings were obtained at 1 to 2 h after infarction. The pressure catheter was withdrawn, all indwelling lines were sealed and the animals allowed to recover from surgery and anesthesia. Parenteral antibiotics (penicillin G [6,000 U]/streptomycin [0.75 g], Tech America) were administered daily for 1 week.

Follow-up data were obtained at 24 h and 1 week after infarction. For each follow-up study, the dogs were anesthetized with thiamylal-Na (100 mg/kg), the pressure transducer catheter was advanced to the left ventricle through the left atrial cannula and biplane cineradiograms with synchronized left ventricular pressure recordings were obtained. All analog data were recorded on a six channel chart recorder (Gould, model 260).

Postmortem analysis. At the end of the study, the animals were killed and the heart removed and weighed. Single plane X-ray films of each heart were taken in several views to provide precise correspondence maps between the actual beads and the planar images. These were used to match beads to the computer-reconstructed markers.

The extent of transmural infarction was determined by gross inspection of unstained 1 cm thick short-axis slices (five to six per heart). Each heart slice was weighed and

measured by planimetry (Hewlett Packard digitizer, model 9864A) and infarct size was calculated as percent of total left ventricular mass. The precise bead position within and remote to the infarct was assessed.

Reconstruction of bead coordinates. The computer bead-tracking and three-dimensional coordinate reconstruction system has previously been described in detail (25). Briefly, in addition to the anteroposterior and lateral views filmed at each study point, cineradiographic records were taken of a calibration cube and lattice grid. The cube data, containing 12 markers at precise locations, enabled computer calculations of the distances between anteroposterior and lateral X-ray sources and their respective image intensifiers. Bead coordinates were calibrated in centimeters. The grid consisted of a 10 × 10 lattice of markers, which was used to define the warping effects of the X-ray lens and permit mathematical dewarping of the digitized images. Biplane views of the calibration cube, grid and bead images were digitized (DeAnza image array processor, model IP660) using a semiautomated tracking algorithm, and the two-dimensional coordinates for each frame and view were stored for processing. The anteroposterior and lateral views were synchronized, and projections of the beads in each view were sequentially paired to generate estimates of the three-dimensional positions of the respective markers. Overall accuracy of the computer analysis was ± 0.1 mm. Calculations were performed using a PDP 11/34 computer.

After the XYZ coordinates for each marker bead in each frame were determined, the computer-reconstructed images were matched to the actual markers on the heart using the reference X-ray projections recorded postmortem. Calculations of neighboring interbead distances disclosed any mispairing, which was easily corrected.

Figure 1. Schematic illustration of epicardial marker placement to determine regional surface areas. Multiple markers are placed within both remote and infarct (ischemic) territories. The area encompassed by three neighboring markers, which define surface triangles, is calculated. The sum of these areas (average of four per region) provides an estimate of the regional surface area and is used as the measure of regional deformation.

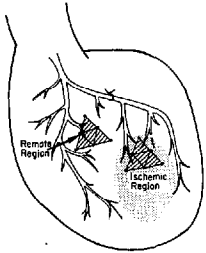

Beads within both remote and infarcted territories (mean five to six beads per region) were identified. Only beads that lay within the dense transmural infarct zone were used for the infarct data, while remote markers were at least 2 cm distant to the infarct border. The exact number of beads that satisfied these criteria varied with the ultimate infarct size and distribution and, therefore, was determined postmortem. Epicardial deformation was determined by calculating the area contained within multiple bead triplets in each zone, and summing each triangle area to generate a regional surface area (Fig. 1). The surface area (SA) of each individual triangle was calculated (MV8000, Data General) directly from the three-dimensional XYZ coordinates of each corner bead (1–3) by the equation:

$$SA(cm^2) = 1/2 \times \left(\begin{vmatrix} 1 & X1 & X2 \\ 1 & Y1 & Y2 \\ 1 & Z1 & Z2 \end{vmatrix}^2 + \begin{vmatrix} 1 & X2 & X3 \\ 1 & Y2 & Y3 \\ 1 & Z2 & Z3 \end{vmatrix}^2 + \begin{vmatrix} 1 & X1 & X3 \\ 1 & Y1 & Y3 \\ 1 & Z1 & Z3 \end{vmatrix}^2 \right)^{1/2}.$$

The surface areas were synchronized with the digitized left ventricular pressures using the electronic signal that identified the timing of each frame. End-diastolic surface area (EDA) was measured at the inflection point of the diastolic ventricular pressure tracing when the first derivative of left ventricular pressure (dP/dt) exceeded a threshold of 10% of maximal (dP/dt_{max}). End-systolic area (ESA) was chosen 20 ms before peak negative dP/dt. This was synchronous with the upper left corner of a pressure-area loop determined within the noninfarcted zone. Percent fractional area shortening (%FAS) was calculated as (EDA−ESA)/EDA × 100.

Statistical analysis. Data are presented as mean ± standard error of the mean. Comparisons between means were performed using analysis of variance with repeated measures, with the Bonferoni correction for multiple comparisons. Because the control values for surface area dimensions varied between the two regions and from dog to dog depending on the eventual size and location of the infarct, analysis was performed on data normalized to the control values; 95% confidence limits were determined using corrections of the pooled variance. One week data were obtained in six of the eight dogs; therefore, statistical comparisons between the 1 week measurements and the earlier time points utilized data only from these six dogs. Statistical significance is reported at the $p < 0.05$ level.

Results

All eight dogs survived at least 36 h after infarction, and seven of the eight survived at least 1 week. However, data at the 1 week point were not obtained in two dogs because of

JACC Vol. 11, No. 1
January 1988:177-85

Table 1. Left Ventricular Mass and Infarct Size in Eight Dogs

	Dog	Site	Mass (g)	% Infarct
	1	LCx	80.0	25
	2	LCx	71.6	29
	3	LCx	102.7	12
	4	LCx	116.8	28
	5	LAD	92.0	22
	6	LCx	84.2	24
	7	LCx	117.5	19
	8	LAD	86.0	25
Mean	—	—	93.8	23.0
± SEM	—	—	5.6	1.8

LAD = left anterior descending coronary artery occlusion; LCx = left circumflex artery occlusion.

technical failure of radiographic equipment in one dog and death from ventricular arrhythmia in the other.

Infarct size (Table 1). Each ventricle displayed gross pathologic evidence of transmural infarction. The circumflex artery infarcts were located within the lateral or posterolateral wall, while the two left anterior descending artery infarcts were located in the distal anteroapical and septal walls. The ventricular mass and site and relative infarct size for each heart are provided in Table 1. The extent of infarction averaged 23 ± 1.8% of left ventricular mass. Seven of the hearts sustained an infarct of 20 to 30% of ventricular cavity size, while one heart had a smaller infarct (12%). Because of variability in the state of contracture postmortem, morphologic studies based on wall thinning and local radius of curvature were not made.

Hemodynamic data (Table 2). End-diastolic pressure increased significantly from 6.0 ± 1.0 to 10.3 ± 0.8 mm Hg immediately after infarction, increased further to 14.8 ± 0.8 at 24 h and remained significantly elevated at 1 week. Although small changes in heart rate, maximal left ventricular pressure and dP/dt_{max} were observed, particularly with acute infarction, none of these other changes achieved statistical significance.

Regional epicardial surface deformation: acute response (Tables 3 and 4). Immediately after myocardial infarction, nearly all of the epicardial surface area triangles in both remote and infarct territories demonstrated significant increases in end-diastolic area, as well as changes in fractional shortening. There were substantial differences, however, between the extent of the increase between the two regions, with a disproportionate degree of dilation within the infarct territory. Table 3 provides the raw data for the remote and infarct territories for all eight dogs. Regional surface area (cm^2) at end-diastole and end-systole and percent fractional area shortening are given. Table 4 provides the end-diastolic area in the two regions normalized to the control values for each dog.

By 1 h after infarction, the normalized end-diastolic area in the infarct region increased to 1.20 ± 0.031, whereas the increase in the remote territory was much less (1.08 ± 0.035). The increases in both regions as well as the difference between them (12.4 ± 2.7% greater dilation in infarct over remote region) were significant. At 24 h, both regions displayed further significant increases in end-diastolic area, but the extent of additional change (10.3 ± 2.8% for remote region, 10.1 ± 2.1% for infarct region) was similar. This more proportionate increase was present in nearly every dog and not just in the mean data. Figure 2 displays the difference between the net percent increase of end-diastolic area in the infarct region versus that in the remote region. All dogs demonstrated a greater percent increase in end-diastolic area within the infarct region at 1 h. This disparity underwent little subsequent change after an additional 24 h in all but one dog.

Figure 3 displays an example (Dog 6) of the response to infarction in the form of pressure-surface area loops. Control loops in both regions were directed counterclockwise, indicating positive regional work. In the infarct territory (panel A), the largest rightward shift (indicating regional dilation) occurred at 1 hour after infarction, and there was relatively little further change for the remainder of the study. The remote region (panel B) also displayed a rightward shift after infarction; however, it was substantially smaller than that observed in the infarct zone. Remote regional stroke work increased acutely, consistent with the increase in end-diastolic area (Frank-Starling effect) and increased further by 24 h after infarction, but then was reduced at 1 week.

Chronic infarct response. Data were obtained 1 week after infarction in six of the eight dogs. The percent change in end-diastolic area and percent fractional area shortening for both the acute and chronic phases of the study are shown for this subset in Figure 4. The acute and 24 h responses in

Table 2. Mean Hemodynamic Responses Before and After Infarction in Eight Dogs

	Control	Inf-1 h	Inf-2 h	Inf-1 wk*
EDP (mm Hg)	6.0 ± 1.0	10.3 ± 0.8†	14.8 ± 0.8†	11.7 ± 1.5†
Peak LVP (mm Hg)	125.2 ± 8.9	116.5 ± 5.7	138.4 ± 9.3	122.1 ± 6.3
dP/dt_{max}	3,201 ± 467	2,541 ± 282	3,519 ± 428	2,964 ± 306
Heart rate (min^{-1})	160 ± 10	170 ± 9	176 ± 7	170 ± 15

*n = 6; †p < 0.05 compared to control. dP/dt_{max} = maximal first derivative of left ventricular pressure; EDP = end-diastolic pressure; Inf-1 h, Inf-24 h and Inf-1 wk = postinfarction at 1 h, 24 h and 1 week, respectively; LVP = left ventricular pressure.

both the remote and infarct territories were similar to those seen for the entire group of study dogs. By 24 h after infarction, end-diastolic area in the infarct territory had increased by a mean of 29.7 ± 2.9% compared with only 16.8 ± 6.3% in the remote region. At 1 week after infarction, the infarct territory remained dilated, with a mean increase of 31.5 ± 3.4% above control end-diastolic area, while the remote region underwent a reduction in dilation, leaving a net increase of only 8.7 ± 5.3%. This resulted in the largest disparity of regional dilation between remote and infarct territories. In Figure 5 the mean percent change in end-diastolic area in the infarct region is plotted against the mean change in the remote region for the six dogs. Early (1 h) disproportionate infarct dilation, with the slope falling far below the line of identity, was followed by more proportionate increases between 1 and 24 h after infarction, more consistent with generalized volume dilation. At 1 week, each dog demonstrated persistent infarct dilation and the extent of remote enlargement underwent a significant reduction.

Discussion

This study demonstrates that marked disproportionate infarct dilation is an acute phenomenon present within 1 h of transmural injury. Continued enlargement occurs over the first 24 h and is associated with remote and presumably global dilation. Compensation begins after this initial period, leading to a significant reduction in the extent of early

Table 3. Response of Epicardial Surface Area in the Remote and Infarct Regions Before and After Infarction

		Dog No.							
	Mean ± SEM	1	2	3	4	5	6	7	8
Remote Region									
C									
EDA	3.61 ± 0.37	4.98	3.29	2.24	4.03	2.61	4.1	4.92	2.75
ESA	3.42 ± 0.36	4.63	2.98	2.07	3.90	2.48	4.04	4.72	2.56
%FS	5.5 ± 0.92	7.1	9.3	7.6	3.0	5.0	1.5	4.0	6.8
I									
EDA	3.91 ± 0.43	5.85	3.67	2.23	4.41	3.25	4.25	5.05	2.58
ESA	3.58 ± 0.42	5.25	3.30	1.96	4.17	2.82	3.88	4.93	2.37
%FS	8.7 ± 1.2*	10.2	10.0	12.1	5.3	13.1	8.7	2.4	8.0
24I									
EDA	4.28 ± 0.49*	6.77	4.00	2.69	4.74	3.33	5.00	5.07	2.68
ESA	3.92 ± 0.47*	6.35	3.39	2.38	4.45	3.11	4.23	4.94	2.53
%FS	8.6 ± 1.7*	6.2	15.1	11.6	6.1	6.5	15.3	2.5	5.4
WKI									
EDA	4.07 ± 0.60	6.11	3.58	2.49	—	—	4.82	4.91	2.50
ESA	3.81 ± 0.58	5.65	3.38	2.20	—	—	4.76	4.59	2.29
%FS	6.3 ± 1.1	7.5	5.5	9.0	—	—	1.2	6.4	8.2
Infarct Region									
C									
EDA	3.86 ± 0.67	5.84	2.53	1.67	6.17	3.06	4.34	5.70	1.53
ESA	3.63 ± 0.65	5.38	2.28	1.45	6.04	3.00	4.18	5.25	1.44
%FS	6.6 ± 1.4	7.9	10.1	13.1	2.1	2.1	3.7	7.9	5.95
I									
EDA	4.60 ± 0.77*	7.30	3.14	1.84	6.73	4.18	5.32	6.45	1.82
ESA	4.68 ± 0.78*	7.35	3.27	1.80	6.68	4.03	5.69	6.69	1.91
%FS	−1.7 ± 1.3*	−0.7	−4.2	1.9	0.7	3.6	−6.9	−3.7	−4.6
24I									
EDA	4.96 ± 0.82*	7.77	3.33	2.22	7.45	4.38	5.91	6.70	1.93
ESA	5.12 ± 0.85*	8.05	3.52	2.22	7.67	4.30	6.21	6.98	2.03
%FS	−3.1 ± 0.95*	−3.6	−5.7	0.0	−2.9	1.8	−5.1	−4.2	−5.2
WKI									
EDA	4.71 ± 1.0*	8.06	3.53	2.15	—	—	5.73	6.75	2.02
ESA	4.78 ± 1.1*	8.33	3.37	2.20	—	—	5.88	6.91	1.96
%FS	−0.7 ± 1.4*	−3.3	4.6	−3.3	—	—	−2.6	−2.4	3.1

*$p < 0.05$ compared with control.

All data are reported as cm^2. C = control; EDA = end-diastolic area; EDS = end-systolic area; %FS = fractional shortening; I = infarct (1 h); 24 I = infarct (24 h); WKI = infarct (1 week).

JACC Vol. 11, No. 1
January 1988:177-85

Table 4. Change in End-Diastolic Area for Each Dog in Both Remote and Infarct Regions

Dog No.	Inf-Acute	Inf-24 h	Inf-1 wk
	Remote Region		
1	1.18	1.36	1.23
2	1.12	1.22	1.09
3	0.99	1.20	1.11
4	1.09	1.18	—
5	1.25	1.28	—
6	1.04	1.22	1.18
7	1.03	1.03	0.99
8	0.94	0.97	0.91
Mean	1.08*	1.18*†‡	1.085*‖
± SEM	0.035	0.044	0.047
	Infarct Region		
1	1.25	1.33	1.38
2	1.24	1.32	1.39
3	1.10	1.33	1.28
4	1.10	1.22	—
5	1.37	1.43	—
6	1.23	1.36	1.32
7	1.13	1.18	1.18
8	1.21	1.26	1.33
Mean	1.20*†	1.30*†‡	1.31*†
± SEM	0.031	0.029	0.031

*$p < 0.05$ compared with opposing region (remote versus infarct); †$p < 0.05$ compared with control; ‡$p < 0.05$ compared with acute infarct response (same region); ‖$p < 0.05$ compared with Inf. 24 h in remote region. Abbreviations as in Table 2. Data are expressed normalized to the control values.

dilation of noninfarcted myocardium. However, infarct dilation remains largely unchanged; thus, the disparity in end-diastolic area between injured and noninjured territories can be increased during this chronic compensatory period.

Figure 2. Disproportionate regional dilation in eight dogs as assessed by the difference between the percent change in end-diastolic surface area (EDA) in the infarct zone minus the change in the remote zone. At 1 h after infarction (acute infarct), all of the data display a positive upward trend, indicating disproportionate infarct dilation. Between 1 and 24 h after infarction, most of the animals show a much smaller change, with no net change in the overall extent of disparity between the two regions.

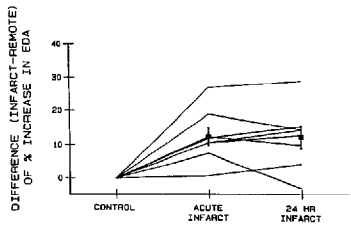

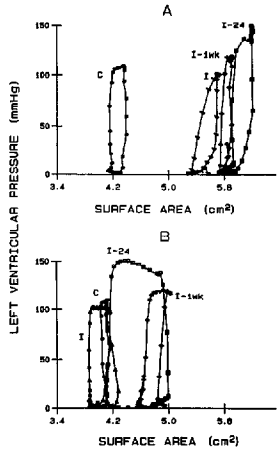

Figure 3. Pressure-surface area loops within the infarct region (A) and remote region (B) for Dog 6. Data for control [(C) ○], 1 h infarct [(I) ▼], 24 h infarct [(I-24) □] and 1 week infarct [(I-1wk) ◇] are shown. Control loops were directed counterclockwise in both regions. With acute infarction, there was a large rightward shift in the pressure-area loop in the infarct region and the loop direction was reversed. A concomitant much smaller shift was seen in the remote territory. Initial disproportionate infarct dilation was maintained throughout the remainder of the study.

Choice of model. Despite many short- and long-term studies on the influence of ischemia on regional wall motion and dimensions, in vivo data from experimental models of transmural infarction are limited. Most canine studies (6,7,17–19) have utilized coronary ligation to induce ischemic injury. However, Eaton and Bulkley (5) demonstrated in the dog that this procedure rarely leads to transmural injury (<10% of cases), and is not accompanied by postmortem morphologic evidence of infarct expansion. Similarly, data from the rat (2,16,22) and human heart (23) have shown that transmural injury is a critical predisposing variable toward the development of chronic disproportionate infarct dilation. With coronary ligation alone, Theroux et al. (6,18) reported that the early increases in subendocardial and end-diastolic segment length within the infarct had completely returned to baseline at 1 week. Others (7,17,20,21) have also reported similar reversals of initial end-diastolic wall thinning or volume enlargement after 1 week of infarction. By combin-

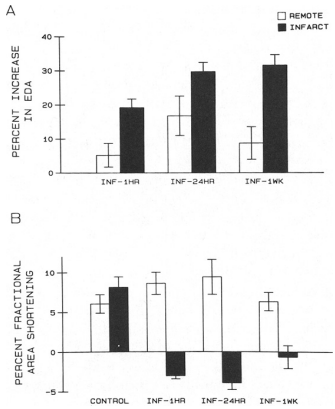

Figure 4. **A,** Percent increase in regional end-diastolic area (EDA) in remote and infarct territories in six dogs. End-diastolic area increased more than twice as much in the infarct (INF) region compared with the remote region by 1 h after the onset of injury. This disproportionality was maintained at 24 h, with further increases in both regions; however, it increased further at 1 week as a result of reductions in the remote region. **B,** Percent fractional shortening of regional surface area in both remote and infarct territories. Systolic bulging (negative fractional shortening) of the infarct region was accompanied by significant increases in fractional shortening in the remote region at 1 and 24 h after infarction. At 1 week, remote fractional area shortening had returned to control levels.

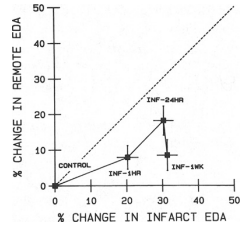

Figure 5. Percent change in end-diastolic area (EDA) of the infarct (INF) versus the remote region. Mean data (± SEM) shown are from the six dogs in which 1 week data were obtained. The dashed line indicates the line of identity and represents "proportional" regional identity.

ing ligation with embolization to minimize collateral flow, we produced a consistent and moderate-sized transmural infarct, which led to persistent infarct dilation at 1 week. Transmural injury enabled the use of epicardial measurements to assess regional deformation after infarction. In addition, and in contrast to most studies in the rat model, our preparation provided longitudinal in vivo measurements of regional deformation.

Disproportionate infarct dilation. Acute ischemia leads to rapid increases in regional myocardial wall dimensions, often with a greater change in the ischemic territory (6,8,26,27). Previous infarct expansion studies in both animals and humans have demonstrated significant ventricular remodeling after ≥24 h. Our data suggested that the major disparities between regional increases in end-diastolic area in the infarct compared with remote region occurred even earlier than previously shown.

The relative disparity observed at 1 h after infarction remained similar at 24 h, even though both regions had undergone further dilation. In a recent canine study, Akaishi et al. (27) reported significantly greater increases of subendocardial end-diastolic length in ischemic compared with nonischemic zones after 15 min of coronary occlusion. When they varied ventricular volume, they found a strong correlation between end-diastolic length changes in each region, with persistent disproportionate lengthening of the ischemic zone. Our data (Fig. 5) similarly suggest that, once established, the disproportionality relation between the extent of increase in epicardial end-diastolic area of infarct compared with noninfarct regions is maintained over the next 24 h, consistent with a generalized chamber volume increase.

The impact of this early chamber enlargement becomes apparent in the chronic infarct data. The changes in end-diastolic area observed at 1 week no longer suggest a simple global volume reduction, but rather chronic remodeling with retained infarct dilation at the level observed 24 h after infarction despite somewhat reduced dimensions in the remote region. The potential for the chronically infarcted heart to decrease in end-diastolic volume has been noted previously (20,21), and may partially explain the increased end-diastolic thickness and reduced end-diastolic length seen in several long-term studies (6,7,17). Increased stiffness of the chronic infarct (28,29) may reverse the initial rightward shift of the diastolic pressure-volume relation (30), increasing the ventricular pressure at the same end-diastolic volume. At the same time, the systolic disadvantage posed by a compliant dyskinetic region (11,12) is reduced by increased infarct stiffness. These changes would enable a reduction of the early increase in end-diastolic volume, with the heart relying less on the Frank-Starling mechanism in maintaining cardiac output. Our data are consistent with this

JACC Vol. 11, No. 1
January 1988:177-85

hypothesis, and further suggest that the capacity to return to smaller chamber dimensions with infarct evolution is greater in noninjured myocardium than it is in the infarct scar itself. Thus, the chronic infarct becomes even more dilated as compared with remote regions, increasing the degree of disproportionate expansion.

The capacity of noninfarcted myocardium to return to smaller chamber dimensions is likely influenced by the extent of tissue damage (11,21). In the rat model (1,2), significant wall thinning and morphologic infarct dilation is most apparent after infarcts >35% of left ventricular mass. When examined at 1 week, these hearts display a persistent general chamber enlargement and have diastolic pressure-volume relations that remain markedly shifted to the right (1). Data from clinical studies (3,10) have also demonstrated continued chamber enlargement in addition to disproportionate infarct dilation when the region of injury is large. Even by using embolization in addition to coronary ligation, the infarcts in our study did not exceed 30% of the left ventricular muscle mass and were smaller than those observed in the rat model. Likely related to this smaller extent of infarction, the remote myocardium better compensated for the infarct injury without leading to continued chronic chamber enlargement. Thus, even with this more "compensated" model of chronic transmural infarction, disproportional infarct dilation changes were prominent. This suggests that some degree of infarct remodeling likely occurs in many, if not all, transmural infarctions. Its extent and eventual influence on chronic ventricular function depends on the size of the injury and the ultimate capacity of adaptive mechanisms.

One potential cause of disparities in the extent of dilation among different regions of the heart after infarction is intrinsic inhomogeneity of chamber wall deformation associated with global volume changes. LeWinter et al. (31) found that with aortic occlusion, mid wall end-diastolic length increased more when measured at the apex than at the base. When examined in the epicardial layer, however, no significant differences were seen. More recently, Lew and LeWinter (32) reported apparent greater diastolic distensibility of anterior versus posterior mid wall segments, which may in part relate to regional geometric differences. However, in the present study, the majority of the infarcts were produced in the lateral or posterolateral wall. The disproportionate extent of dilation in this region after infarction occurred despite the greater intrinsic potential for distension in the anteroapical region with generalized dilation.

End-diastolic area versus end-diastolic length. Nearly all previous in vivo investigations of the changes after acute and chronic infarction have used some variation of segment length or wall thickness to describe regional deformation. Although there are some advantages to the use of wall thickness measurements, since the data express changes throughout the wall, there are also several disadvantages to the use of these measures in describing ventricular remodeling. One disadvantage relates to the limited sample size of a single segment length or thickness measurement. Inhomogeneities in both infarct and remote regions are likely to be present so that a single measurement can under- or overrepresent the extent of change occurring over a larger region. By using multiple surface triangles, we incorporated data over a larger area of the heart and reduced the influence of local inhomogeneity.

A second problem of single dimension measurements relates to the orientation of the measurement. Differences in the extent of change in end-diastolic length may vary depending on the orientation of the segment. This has been reported with subendocardial ischemia (33), where substantially different epicardial responses were seen in circumferential versus longitudinal orientations within a region with the endocardium made ischemic. Although this problem may be less significant with transmural infarction, the directional influence on data from the remote region would still be present on the epicardial surface. By using area rather than length, we sought to reduce the influence of any one direction by offsetting it with the two other directions in each triangle.

Limitations. There are several limitations in the present study. We were not able to measure or control end-diastolic volume, so the absolute extent of epicardial surface area changes after infarction were related to both regional remodeling and global changes in chamber volumes. Differences in the hydration status of each animal, therefore, probably contributed to the variability in the observed dilation changes. End-diastolic pressure cannot be used in this regard because the diastolic chamber properties change with infarct evolution. However, the major focus of the study was on the relative differences between two regions of the same heart and, thus, absolute volume control was not essential.

Differences in the anesthetic agent used for the acute data (pentobarbital) compared with the chronic data (thiamylal) could account for small differences between the measurements. However, both agents are similarly vagolytic and have similar effects on blood pressure and heart rate; therefore, this difference was unlikely to significantly influence the results.

It is possible that, with infarction, some degree of random migration of epicardial markers occurred during the period of maximal necrosis. This is unlikely, however, because the pattern of interbead distances was quite consistent throughout the study, and closely resembled the 1 h response before necrosis was likely to be present. More importantly, by measuring surface area of multiple triangles, small deviations in any given bead position would have less influence on the total area because one triangle would compensate for another, unless all of the beads migrated in a consistent manner. However, this would no longer represent random migration.

Conclusions. We demonstrated that a significant extent of disproportionate infarct dilation occurs within 1 h of transmural injury in the dog. Generalized dilation that continues over the ensuing 24 h further increases the degree of infarct enlargement; however, the disproportionality remains essentially unchanged. With chronic infarct maturation, the remote region returns toward normal dimensions whereas the infarct remains dilated, producing the maximal disparity between normal and infarct regions. Thus, very early disproportionate dilation appears to determine the extent of late infarct remodeling. However, some amount of initial chamber enlargement is related to compensatory mechanisms used in maintaining cardiac output. Interventions aimed at limiting the extent of late infarct dilation by ventricular unloading must balance with the compensatory role of acute global chamber enlargement.

References

1. Fletcher PJ, Pfeffer JM, Pfeffer MA, Braunwald E. Left ventricular diastolic pressure-volume relations in rats with healed myocardial infarction. Circ Res 1981;49:618–26.
2. Weisman HF, Bush DE, Mannisi JA, Bulkley BH. Global cardiac remodeling after acute myocardial infarction: a study in the rat model. J Am Coll Cardiol 1985;5:1355–62.
3. Eaton LW, Weiss JL, Bulkley BH, Garrison JB, Weisfeldt ML. Regional cardiac dilation after acute myocardial infarction. N Engl J Med 1979;300:57–62.
4. Vokonas PS, Pirzada FA, Hood WB Jr. Experimental myocardial infarction. XII. Dynamic changes in segmental mechanical behavior of infarcted and non-infarcted myocardium. Am J Cardiol 1976;37:853–9.
5. Eaton LW, Bulkley BH. Expansion of acute myocardial infarction: its relationship to infarct morphology in a canine model. Circ Res 1979;49:80–8.
6. Theroux P, Franklin D, Ross J Jr, Kemper WS. Regional myocardial function during acute coronary artery occlusion and its modification by pharmacologic agents in the dog. Circ Res 1974;35:896–908.
7. Sasayama S, Gallagher KP, Kemper WS, Franklin D, Ross J Jr. Regional left ventricular wall thickness early and late after coronary occlusion in the conscious dog. Am J Physiol 1981;240:H293–9.
8. Lew WY, Ban-Hayashi E. Mechanisms of improving regional and global ventricular function by preload alterations during acute ischemia in the canine left ventricle. Circulation 1985;72:1125–34.
9. Heikkila J, Tabakin BS, Hugenholtz PG. Quantification of function in normal and infarcted regions of the left ventricle. Cardiovasc Res 1972;6:516–31.
10. McKay RG, Pfeffer MA, Pasternak RC, et al. Left ventricular remodeling after myocardial infarction: a corollary to infarct expansion. Circulation 1986;74:693–702.
11. Bogen DK, Rabinowitz SA, Needleman A, McMahon TA, Abelman WH. An analysis of the mechanical disadvantage of myocardial infarction in the canine left ventricle. Circ Res 1980;47:728–41.
12. Tyson K, Mandelbaum I, Shumacker HB Jr. Experimental production and study of left ventricular aneurysms. J Thorac Cardiovasc Surg 1962;44:731–7.
13. Schuster EH, Bulkley BH. Expansion of transmural myocardial infarction: a pathophysiologic factor in cardiac rupture. Circulation 1979;60:1532–8.
14. Erlebacher JA, Weiss JL, Weisfeldt ML, Bulkley BH. Early dilation of the infarcted segment in acute transmural myocardial infarction: role of infarct expansion in acute left ventricular enlargement. J Am Coll Cardiol 1984;4:201–8.
15. Meizlish JL, Berger HJ, Plankey M, Errico D, Lew W, Zaret BL. Functional left ventricular aneurysm formation after acute anterior transmural myocardial infarction. N Engl J Med 1984;311:1001–16.
16. Roberts CS, Maclean D, Maroko P, Kloner RA. Early and late remodeling of the left ventricle after acute myocardial infarction. Am J Cardiol 1984;54:607–10.
17. Roan PG, Buja M, Izquierdo C, Hashimi H, Shaffer S, Willerson JT. Interrelationships between regional left ventricular function, coronary blood flow, and myocellular necrosis during the initial 24 hours and 1 week after experimental coronary occlusion in awake, unsedated dogs. Circ Res 1981;49:31–40.
18. Theroux P, Ross J Jr, Franklin D, Covell JW, Bloor CM, Sasayama S. Regional myocardial function and dimensions early and late after myocardial infarction in the unanesthetized dog. Circ Res 1977;40:158–65.
19. Roan P, Scales F, Saffer S, Buja LM, Willerson JT. Functional characterization of left ventricular segmental responses during the initial 24 h and 1 wk after experimental canine myocardial infarction. J Clin Invest 1979;64:1074–88.
20. Weisse AB, Saffa RS, Levinson GE, Jacobson WW, Regan TJ. Left ventricular function during the early and late stages of scar formation following experimental myocardial infarction. Am Heart J 1970;79:370–83.
21. Hood WB. Experimental myocardial infarction. III. Recovery of left ventricular function in the healing phase: contribution of increased fiber shortening in noninfarcted myocardium. Am Heart J 1970;79:531–8.
22. Weisman HF, Bush DE, Mannisi JA, Bulkley BH. Effect of extent of transmurality on infarct expansion (abstr). Clin Res 1984;32:477A.
23. Pirolo JS, Hutchins GM, Moore GW. Infarct expansion: pathologic analysis of 204 patients with a single myocardial infarct. J Am Coll Cardiol 1986;7:547–54.
24. Shoukas AA, Sagawa K, Maughan WL. Chronic implantation of radiopaque beads on endocardium, midwall, and epicardium. Am J Physiol 1981;241:H104–7.
25. Garrison JB, Ebert WL, Jenkins RE, et al. Measurement of three-dimensional positions and motions of large numbers of spherical radiopaque markers from biplane cineradiograms. Comput Biomed Res 1982;15:76–96.
26. Lew YW, Chen Z, Guth B, Covell J. Mechanisms of augmented segment shortening in nonischemic areas during acute ischemia of the canine left ventricle. Circ Res 1985;56:351–8.
27. Akaishi M, Weintraub WS, Schneider RM, Klein LW, Agarwal JB, Helfant RH. Analysis of systolic bulging: mechanical characteristics of acutely ischemic myocardium in the conscious dog. Circ Res 1986;58:209–17.
28. Hood WB, Bianco JA, Kumar R, Whiting RB. Experimental myocardial infarction. IV. Reduction of left ventricular compliance in the healing phase. J Clin Invest 1970;49:1316–23.
29. Connelly CM, Vogel WM, Wiegner AW, et al. Effects of reperfusion after coronary artery occlusion on post-infarction scar tissue. Circ Res 1985;57:562–77.
30. Forrester JS, Diamond G, Parmley WW, Swan HJC. Early increase in left ventricular compliance after myocardial infarction. J Clin Invest 1972;51:598–603.
31. LeWinter MM, Kent RS, Kroener JM, Carew TE, Covell JW. Regional differences in myocardial performance in the left ventricle of the dog. Circ Res 1975;37:191–9.
32. Lew WYW, LeWinter MM. Regional comparison of midwall segment and area shortening in the canine left ventricle. Circ Res 1986;58:678–91.
33. Gallagher KP, Osakada G, Hess OM, Koziol JA, Kemper WS, Ross J Jr. Subepicardial segmental function during coronary stenosis and the role of myocardial fiber orientation. Circ Res 1982;50:352–9.